^{55}Mn NMR in Mn_{12} acetate: Hyperfine interaction and magnetic relaxation of the cluster

T. Kubo*
Physics Department, Faculty of Education, Nara University of Education, Nara 630-8528, Japan

T. Goto and T. Koshiba
Graduate School of Human and Environmental Studies, Kyoto University, Kyoto 606-8501, Japan

K. Takeda
Department of Chemistry, Graduate School of Science, Hokkaido University, Sapporo 060-0810, Japan

K. Awaga
Department of Chemistry, Graduate School of Science, Nagoya University, Nagoya 464-8602, Japan
(Received 11 December 2001; published 10 June 2002)

The ^{55}Mn NMR in oriented powder crystal of $Mn_{12}Ac$ has been investigated at 1.4–2.0 K in zero field and with external fields along the *c* axis. Three kinds of ^{55}Mn NMR composed of fivefold quadrupole-split lines for $I=5/2$ nuclei have been interpreted to arise from a Mn^{4+} ion and two crystallographically inequivalent Mn^{3+} ions. The isotropic hyperfine field in the Mn^{4+} ion indicates a large amount of reduction (26%) as compared with the theoretical evaluation. In the analysis of the hyperfine field in Mn^{3+} ions, the anisotropic dipolar contribution has been taken into account in addition to the Fermi-contact term. Adopting the reduction factor 8% of the dipolar term, which is estimated from the magnetic moment determined by a polarized-neutron-diffraction experiment, we obtained a reduction of 15% for the Fermi-contact term. We suppose that such an appreciable amount of the reduction factor is due to the covalence and strong exchange interaction among manganese ions via the oxygen ions. By using the hyperfine coupling constants of 12 manganese ions in the Mn_{12} cluster, the total hyperfine interaction of the ferrimagnetic ground state of $S=10$ has been determined to amount to 0.3 cm^{-1} in magnitude at most, the magnitude of which corresponds to the nuclear hyperfine field 0.32 kG seen by the cluster spin. The relaxation of the cluster magnetization after reversal of the external field was investigated by observing the recovery of the ^{55}Mn spin-echo intensity in the fields of 0.20–1.90 T along the *c* axis at 2.0 K. The magnetization of the cluster exhibited the square-root *t* recovery in the short-time regime. With increasing external field, the relaxation time decreased following significant dips at every 0.45 T, which is due to the effects of phonon-assisted quantum tunneling between the spin states at magnetic level crossings.

DOI: 10.1103/PhysRevB.65.224425 PACS number(s): 75.50.Xx, 76.60.−k, 75.45.+j, 76.60.Lz

I. INTRODUCTION

Recently, there has been great interest in compounds of nanoscale magnets with a high value of spin involving a large number of magnetic ions.[1–6] This is based on the view of studying the quantum physics of the mesoscopic system, which lies in the intermediate scale between the classical macroscopic and quantum microscopic scales. Among various molecular clusters, $Mn_{12}O_{12}(CH_3COO)_{16}(H_2O)_4$ (abbreviated as $Mn_{12}Ac$) (Ref. 7) has been most extensively studied theoretically[8–16] and also experimentally so far using magnetization,[17–26] ac susceptibility,[27,28] heat capacity,[29,30] neutron scattering,[31–34] electron spin resonance (ESR),[35,36] and proton NMR and muon spin resonance (μSR).[37,38] The most prominent feature is the characteristic magnetization relaxation and the stepwise hysteresis curve associated with the phonon-assisted resonant quantum tunneling.[19,20,39,40]

In $Mn_{12}Ac$, each of the magnetic clusters, which constitute a tetragonal symmetry (S_4), is constructed from four Mn^{4+} ($S=3/2$) ions [the site denoted as Mn(1)] in a central tetrahedron and surrounding eight Mn^{3+} ($S=2$) ions with two crystallographically inequivalent sites [Mn(2) and Mn(3)] which are located alternately in the outer ring.[7] Figures 1(a) and 1(b) show, respectively, the molecular structure viewed from the crystallographical *c* axis and the two inequivalent Mn^{3+} sites surrounded octahedrally by neighboring oxygens together with their local tetragonal axes δ.

The magnetic ground state of $Mn_{12}Ac$ clusters is determined by combined effect of four paths of intramolecular exchange interactions, whose values are estimated as follows in Ref. 18: the dominant interaction between Mn(1) and Mn(2) is antiferromagnetic (-150 cm^{-1}) and the interactions between the neighboring two Mn(1) ions and between Mn(1) and Mn(3) are both also antiferromagnetic (-60 cm^{-1}). The interaction between Mn(2) and Mn(3) is ferromagnetic or antiferromagnetic (less than 40 cm^{-1}). Because of the single-ion anisotropy originating in Mn^{3+} ions due to the Jahn-Teller effect, the cluster totally possesses Ising-like anisotropy along the crystallographic *c* axis. The following model is established experimentally: four Mn^{4+} spins in the inner tetrahedron are parallel to each other ($S=3/2\times4=6$) and eight Mn^{3+} spins in the outer ring are also parallel ($S=2\times8=16$). Then the total spins of the two groups couple antiparallelly to form $S=10$ for the cluster.[17] Most of the

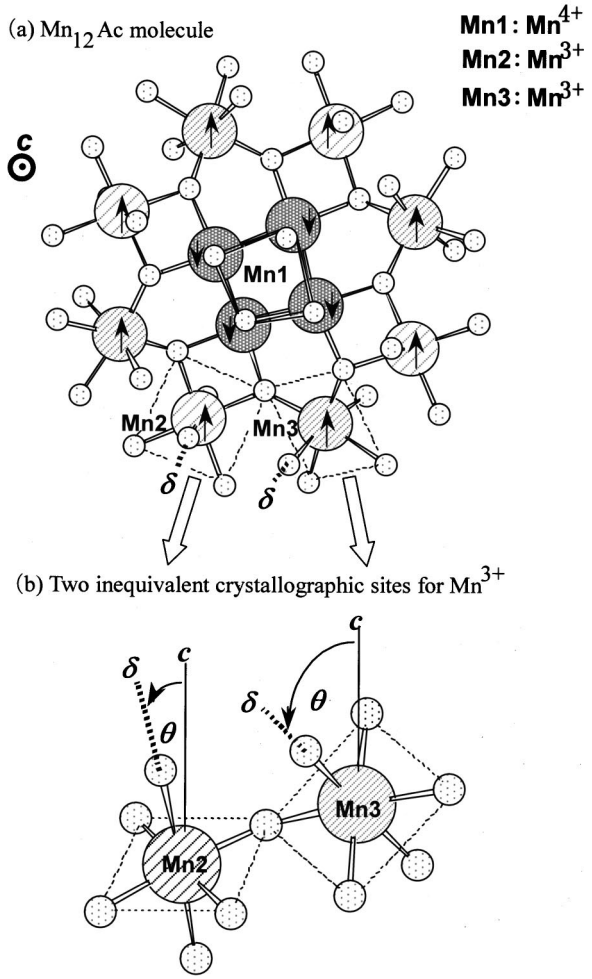

FIG. 1. (a) Schematic molecular structure of $Mn_{12}Ac$ clusters viewed from the c axis, where Mn(1) sites are occupied by Mn^{4+} ions and both Mn(2) and Mn(3) sites by Mn^{3+} ions using Lis' notation (Ref. 7). For clarity in simplifying other ions, manganese ions are represented by large spheres and oxygen ions by small ones. Arrows on manganese sites indicate the directions of their spins that are parallel or antiparallel to the c axis. (b) Two kinds of octahedral environments for crystallographically inequivalent Mn^{3+} ions, where the symmetry around Mn(2) ($\theta=11.7°$) is approximately tetragonal, while the one around Mn(3) ($\theta=36.2°$) is rhombic in addition. The longest axes are denoted by δ for both cases. Dotted squares correspond to the planes where the principal parts of the wave function $|X^2-Y^2\rangle$ expand.

magnetic properties have been well understood in terms of the doubly degenerated discrete energy levels of the cluster with a high spin of $S=10$, which are specified by the wave function $|S,m\rangle$ in terms of the Hamiltonian $\mathcal{H}_0=-DS_z^2$, where the constant D is the effective Ising-like anisotropy of the order of 0.52–0.60 K (Refs. 33 and 35) along the c axis. In addition to this term, it has been recognized that there are the quartic anisotropy energies denoted by $\mathcal{H}'$, the off-diagonal term of which plays an important role for the tunneling, though the magnitude is much smaller as compared with $\mathcal{H}_0$. Then, in the presence of an external field H applied along the c axis, the spin Hamiltonian describing the cluster molecule is given as

$$\mathcal{H}=\mathcal{H}_0-g_z\mu_B S_z H+\mathcal{H}'$$
$$=-DS_z^2-g_z\mu_B S_z H-ES_z^4+B(S_+^4+S_-^4), \qquad (1)$$

where $g_z=1.93$,[35] $E=(1.1-1.3)\times10^{-3}$ K,[32,33,35] and $B=\pm(2.1-7.2)\times10^{-5}$ K.[32,35]

On the other hand, there has been proposed another spin model,[18] which describes the Mn_{12} molecular spin ($S=10$) as being composed of four dimers with $s=1/2$ [an antiferromagnetically coupled pair of Mn(1)-Mn(2)] and four $S=2$ [Mn^{3+} of Mn(3)]. This model has been used for the theoretical interpretation[41,42] of magnetic properties due to a simple description of the exchange interactions.

Considering that the spin structure of the high spin is basically constituted of four Mn^{4+} ions and of eight Mn^{3+} ions, it seems also important to investigate, from the microscopic point of view, the ground state of each manganese ion, in order to understand the nature of the ground state of the cluster. The most prominent experimental procedure for this purpose is to examine ^{55}Mn NMR in $Mn_{12}Ac$. The NMR information on the behavior of manganese ions will be also important to interpret the magnetic relaxation with quantum tunneling at low temperature. From such a viewpoint, we have been studying the ^{55}Mn NMR in $Mn_{12}Ac$. We have already succeeded in observing three kinds of ^{55}Mn NMR for powder crystals of $Mn_{12}Ac$ below 2.4 K in zero external field. In the preliminary paper,[43] we have assigned the lowest ^{55}Mn NMR spectra as due to Mn^{4+} ions, while the higher two ones to crystallographically inequivalent Mn^{3+} ions, and reported the result for the nuclear relaxation time T_2. Subsequently, we investigated the relaxation of magnetization of Mn_{12} cluster by monitoring the spin-echo intensity of Mn^{4+} ions in the external field applied along the c axis.[44]

In the present work we have performed ^{55}Mn NMR measurements in more detail on an oriented-powder sample of $Mn_{12}Ac$ in zero field and with the applied field along the c axis. By considering anisotropic terms of the hyperfine fields due to the dipolar interaction in addition to the Fermi-contract term we have analyzed the hyperfine fields both of Mn^{4+} ions and of two inequivalent Mn^{3+} ions. We have explained the results in an accurate assignment of three kinds of ^{55}Mn NMR spectra to the relevant manganese ions located at Mn(1), Mn(2), or Mn(3) sites, respectively. In order to investigate the behavior of magnetization recovery and quantum tunneling in $Mn_{12}Ac$ we have also measured the relaxation time of the cluster magnetization as a function of the external field, using the spin-echo signal of Mn^{4+} NMR in a field of 0.20–1.90 T along the c axis at 2.0 K.

II. EXPERIMENTAL RESULTS

A. ^{55}Mn NMR

The experiment has been performed by the conventional spin-echo method using a pulsed NMR apparatus. The oriented-powder sample of $Mn_{12}Ac$ contained in a capsule (6 mm diameter and 20 mm in length) is inserted in a resonant cavity of cylindrical shape.

Figure 2 shows the experimental results of ^{55}Mn NMR spectra obtained at 1.4 K in the frequency range between 150

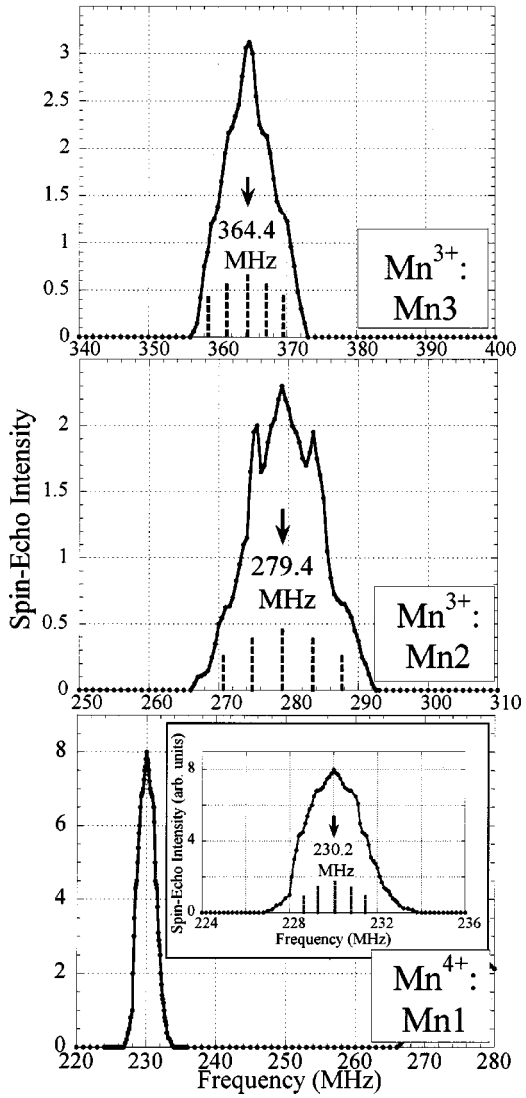

FIG. 2. Three kinds of ^{55}Mn NMR spectra observed in Mn_{12}Ac in zero external field at 1.4 K. The inset shows the enlarged spectra for the Mn^{4+} ions. In every spectra the arrow indicates the central frequency $\nu_{-1/2\leftrightarrow 1/2}$ of fivefold quadrupole-split lines for ^{55}Mn($I=5/2$) nuclei.

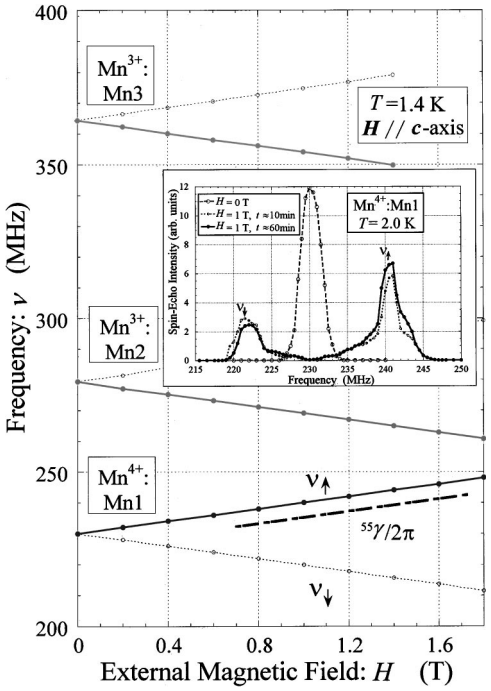

FIG. 3. Frequency-field diagram of three kinds of ^{55}Mn NMR central frequencies in oriented powder Mn_{12}Ac under external fields applied along the *c* axis. When cooled down with ZFC two components (dotted and solid lines) are always observed for the external-field dependence of every central frequency, while with FC a single component (solid lines) is observed only. The inset shows zero-field spectra (dashed line) and the splitting into two components $\nu_{\uparrow}$ and $\nu_{\downarrow}$ observed for Mn^{4+} ions at 1 T. As the time elapses since the field 1 T is applied, the spectra of $\nu_{\uparrow}$ increase a little in intensity, while those of $\nu_{\downarrow}$ decrease, which corresponds to fact that the cluster magnetizations relax to the direction of applied field with upsetting their own magnetic moments.

and 450 MHz in zero external field. Each of the three kinds of ^{55}Mn NMR is composed of fivefold quadrupole-split lines for the $I=5/2$ nucleus. The width of the spectra around 230 MHz is nearly 4 times narrower than those of the others. As we explain in detail in the next section, we assign these three kinds of NMR spectra to manganese nuclei associated with the Mn^{4+} ion and two inequavalent Mn^{3+} ions by taking into account individual resonance profiles such as the central frequency, quadrupole splitting, and field dependence and by considering the anisotropy of the hyperfine field. In this section, we mention briefly the results for the assignment of the three NMR spectra.

The spectra around 230 MHz in Fig. 2 correspond to ^{55}Mn NMR in Mn^{4+} ions at the Mn(1) site. The central frequency is 230.2 ± 0.1 MHz with a quadrupole splitting $\Delta\nu_Q=0.72\pm0.05$ MHz, which can be noticed in the inset. This quite small quadrupole splitting is attributed to the deformation of the crystal field from cubic symmetry for an orbital singlet ion. The resonance frequency corresponds to the hyperfine field $|H_N|=218.4\pm0.1$ kG. On the other hand, in the case of an orbital doublet ion, the NMR spectra show in general relatively large quadrupole splitting coming from the aspherical distribution of the outer electrons. So the two broad spectra are referred to the orbital doublet ion: i.e., the Mn^{3+} ion. As described later in Sec. III, the magnitude of the hyperfine field for the Mn^{3+} ion increases, owing to the anisotropic dipolar contribution, in accordance with an increase in the angle θ between the electron-spin axis and the local tetragonal axis. On the other hand, the quadrupole splitting decreases as the angle θ increases. Since the angle θ is larger in the Mn(3) site than the one for the Mn(2) site, the hyperfine field and hence ^{55}Mn NMR frequency are larger for the Mn^{3+} ion at the Mn(3) site while the quadrupole splitting is smaller. Then we may assign the broad spectra centered at 279.4 ± 0.1 MHz ($|H_N|=264.8\pm0.1$ kG) with $\Delta\nu_Q=4.3\pm0.1$ MHz to the Mn^{3+} ion at the Mn(2) site and the spectra 364.4 ± 0.1 MHz ($|H_N|=345.4\pm0.1$ kG) with $\Delta\nu_Q=2.9\pm0.1$ MHz to the Mn^{3+} ion at the Mn(3) site, respectively.

Figure 3 shows the external magnetic field dependence of

each central line of the above-ascertained ^{55}Mn NMR, which has been measured at 1.4 K in the field H applied along the c axis. We obtained γ values which coincide with that of the free ^{55}Mn nucleus ($^{55}\gamma/2\pi = 1.055$ MHz/kG) within the experimental error. When the specimen is cooled down without an external field [zero-field cooled (ZFC)], we observe two components for every central frequency, i.e., increasing and decreasing branches versus H. The typical NMR spectra of ^{55}Mn NMR in Mn^{4+} ions are shown in the inset to Fig. 3, where the narrow line (dashed line) in the zero field splits into two components $\nu_\uparrow$ and $\nu_\downarrow$ at $H = 1.0$ T after ZFC. However, when the specimen is cooled down below the blocking temperature $T_B = 3$ K with H parallel to the c axis [field cooled (FC)] we observe only one branch expressed by the solid line.

We interpret the present ^{55}Mn NMR frequency-field diagram by considering the magnetic structure of the cluster. Due to the uniaxial anisotropy along the c axis, the magnetic moment of $S = 10$ stays along the c axis even if there is no external field. Because of weak dipolar interaction ($\sim$0.05 K) among neighboring clusters, each molecular cluster, however, remains superparamagnetic. Therefore, when it is cooled down with ZFC the molecular magnets have two possibilities in direction, parallel or antiparallel to the c axis in each crystal. That is the reason why we observed two branches shown by the solid and dotted lines in Fig. 3 in the field dependence of ^{55}Mn NMR in the case of ZFC. On the other hand, when the whole molecular crystals are cooled down in FC, they have a magnetic moment orienting to the unique direction along H, shown in Fig. 4(a). Considering that the ^{55}Mn NMR frequency is proportional to the total field acting on the ^{55}Mn nucleus, the three solid lines in Fig. 3 mean that effective fields acting on ^{55}Mn nuclei in two different Mn^{3+} ions decrease with the external field, while those acting on ^{55}Mn nuclei in Mn^{4+} ions increase. Considering both hyperfine fields to be oppositely directed to their local moments for Mn^{3+} and Mn^{4+} ions, the fact that we observed only the solid lines as shown in Fig. 3 in the case of FC is consistent with the fact that the magnetic moments of the Mn^{3+} ions are parallel to the total moment of the cluster while those of the Mn^{4+} ions are antiparallel,[18] as shown in Figs. 4(a) and 4(c). The situation is explained in detail in Sec. III.

B. Magnetic relaxation of the Mn_{12}Ac cluster

The magnetic relaxation of the cluster was measured after cooling the oriented-powder sample down to 2.0 K from 4.2 K under an applied field of 1.2 T along the c axis. After this FC process, we can observe ^{55}Mn NMR in Mn^{4+} ions at $\nu = 230.4 + (\gamma_{Mn(1)}/2\pi)H = 243.0$ MHz in a field of $H = 1.2$ T, while we cannot observe any signal at $\nu = 230.4 - (\gamma_{Mn(1)}/2\pi)H = 217.8$ MHz. The situation is upset in the case of reversing the field, i.e., we observe ^{55}Mn NMR in Mn^{4+} ions only at $\nu = 217.8$ MHz, while we cannot observe any signal at $\nu = 243.0$ MHz. The reversal of the external field can be reached within a few seconds. Accordingly, by reversing the external field after FC, we can measure the relaxation of the cluster magnetization in the field by probing

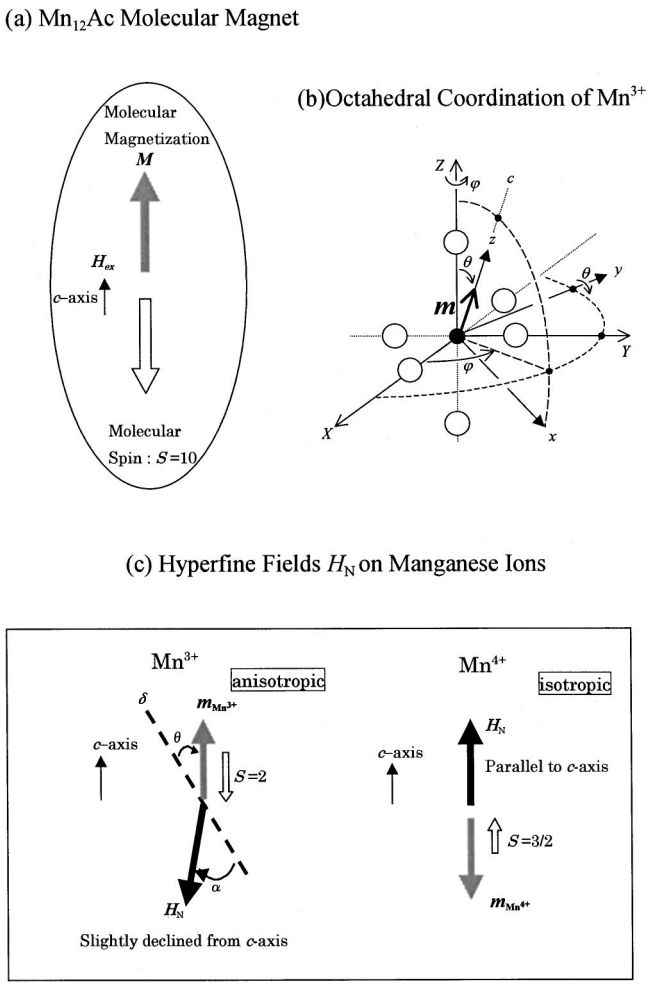

FIG. 4. (a) Stable situation of Mn_{12}Ac molecular magnetization **M** and net spin **S** in the external field applied along the c axis. (b) Schematic illustration of the octahedral coordination of sixfold oxygens around the Mn^{3+} ion at the Mn(2) or Mn(3) site in Mn_{12}Ac, showing the relationship between the two reference frames *XYZ* and *xyz*. The axes *XYZ* are along the principal axes of the crystal field of ligands, while the z axis is chosen along the magnetization **m** of the Mn^{3+} ion [at the Mn(2) or Mn(3) site]. (c) When the molecular magnetization **M** is directed as shown in Fig. 4(a), the mutual relationship of the directions of the magnetic moment **m**, electron spin **S**, and hyperfine field $\mathbf{H}_N$ is schematically shown for Mn^{3+} ions [at Mn(2) or Mn(3) sites] and for Mn^{4+} ions [at Mn(1) sites]. Concerning the Mn^{4+} ion, $\mathbf{H}_N$ is parallel to the external field along the c axis, while that for the Mn^{3+} ion is declined by α-θ from the c axis.

the growth of the spin-echo amplitude of ^{55}Mn NMR in Mn^{4+} ions at $\nu = 243.0$ MHz.[44]

Figure 5 shows the recovery of the spin-echo intensity of $\nu_\uparrow$ branch of ^{55}Mn NMR in the Mn^{4+} ion after reversal of the external field, where the time-dependent growth of the intensity of the $\nu_\uparrow$ line corresponds to the magnetic relaxation of the cluster moment along the applied field. A typical example of the relaxation curve is depicted in Fig. 5, in which the growth of the spin-echo intensity is shown for two values of $H = 1.2$ and 1.4 T at 2.0 K. From the recovery of the signal intensity we can recognize the time dependence of square-root t until about 20 min for 1.2 T and 13 min for 1.4

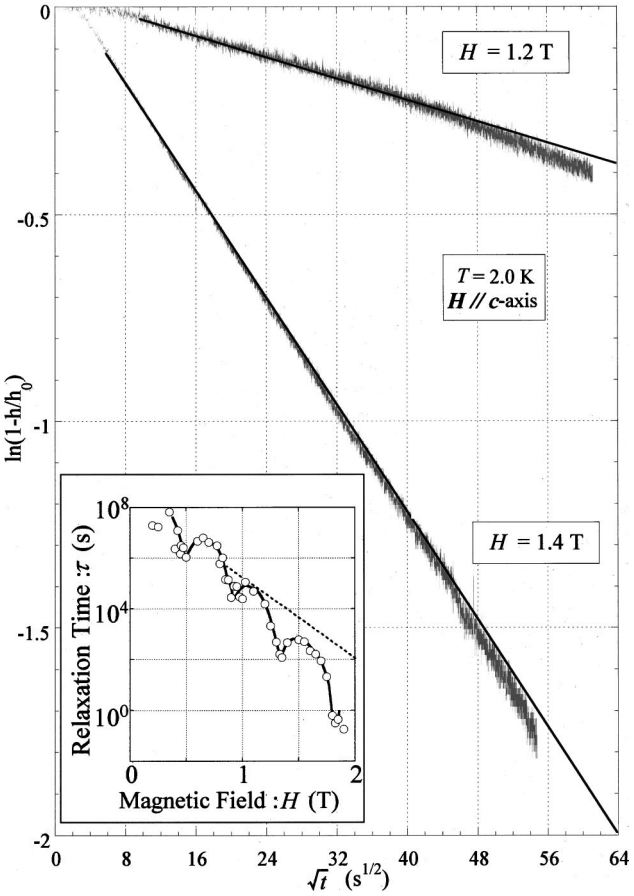

FIG. 5. Semilogarithmic plot of ^{55}Mn spin-echo amplitude of Mn^{4+} ions concerning the $\nu_{\uparrow}$ branch in Fig. 3 vs the square root t that is obtained after reversing the external field for the oriented crystal prepared in FC along the c axis. It is seen that the spin-echo amplitude h follows the function $h=h_0[1-\exp\{-(t/\tau)^{1/2}\}]$ in short times, which corresponds to the magnetization relaxation of the Mn_{12} cluster in the external field. The inset shows the relaxation time τ vs the external field. The solid lines are a guide for the eyes in both figures.

T. From the slope of the square-root t recovery curve we can get the characteristic time τ measured in the early stage of relaxation (short times) as a function of H. In order to see the effect of the quantum tunneling, we performed measurements by changing fields in steps of 0.025 T between 0.200 and 1.900 T. The inset demonstrates that τ not only shows a gradual decrease with increasing the fields, but also shows significant dips of more than one order of magnitude at every 0.45 T-step. Such a feature is obvious above 2.0 K, while below about 1.8 K it is not so clear.

III. HYPERFINE FIELD AND ^{55}Mn NMR

A. Hyperfine field

The hyperfine interaction is composed of both a magnetic hyperfine interaction $\mathcal{H}_n$ with its own electrons and an electrostatic quadrupole interaction $\mathcal{H}_Q$ with surrounding ligands: namely, $\mathcal{H}_{\rm hyp}=\mathcal{H}_n+\mathcal{H}_Q$.[45,46] The effective magnetic hyperfine Hamiltonian is obtained by averaging $\mathcal{H}_n$ with respect to the electronic ground-state wave function ψ_g and can be expressed in terms of the hyperfine field $\mathbf{H}_N$ acting on the nucleus with a nuclear magnetic moment $\gamma\hbar\mathbf{I}$ as follows:[45,47]

$$\langle\psi_g|\mathcal{H}_n|\psi_g\rangle=-\gamma\hbar\mathbf{I}\cdot\mathbf{H}_N=-\gamma\hbar\mathbf{I}\cdot(\mathbf{H}_F+\mathbf{H}_d+\mathbf{H}_l), \quad (2)$$

in which $\mathbf{H}_F$, $\mathbf{H}_d$, and $\mathbf{H}_l$ are Fermi-contact, dipolar, and orbital hyperfine fields resulting from the corresponding components of the magnetic hyperfine interaction.

On the other hand, the effective nuclear-quadrupole Hamiltonian is obtained by the expectation value of $\mathcal{H}_Q$ with respect to ψ_g, as follows:[46]

$$\langle\psi_g|\mathcal{H}_Q|\psi_g\rangle=\frac{e^2Qq_{zz}}{4I(I-1)}\{3I_Z^2-I(I+1)+\eta(I_X^2-I_Y^2)\}, \quad (3)$$

where eQ is a quadrupole moment, eq_{ZZ} is the maximum principal value of the electric field gradient tensor V_{ZZ} along the Z axis,[46] and η is an asymmetry parameter defined by $(V_{XX}-V_{YY})/V_{ZZ}$.

The Fermi-contact field, which is due to core polarization of inner s electrons caused by $3d$-electron spins, is dominant in magnitude ($\approx 10^2$ kG) and opposite in direction to the atomic magnetic moment.[46] The dipolar hyperfine field does not exist in a singlet ion.[45,46] Concerning the orbital hyperfine field, though it is normally zero for the case of an orbital singlet state or of a doublet state due to orbital quenching, it survives slightly when the ground orbital state is admixed with excited states through the spin-orbit interaction and/or low-symmetry crystal field. Since the extent of the mixing corresponds to the g shift, the orbital hyperfine field can be described as[45]

$$H_l=-2\mu_B\langle r^{-3}\rangle\Delta g=-125\langle r^{-3}\rangle_{\rm a.u.}\Delta g \ \ \text{kG}. \quad (4)$$

The ground state of the Mn^{4+} ion ($3d^3$, ^4F) is orbital singlet in a cubic crystal field V_c.[46] Then the dipolar hyperfine field of the Mn^{4+} ion vanishes. It also follows that quadrupole splitting vanishes.[46]

In general, the g factor for Mn^{4+} has been observed to be $\approx$1.99 and $|\Delta g|$ appears normally less than 0.01,[45] so the orbital hyperfine field is evaluated to be less than 10 kG from Eq. (4), using the value $\langle r^{-3}\rangle_{\rm a.u.}=5.36$ expressed in atomic units for free Mn^{4+} ions.[45] Then the orbital hyperfine field can be reasonably neglected compared with H_F. Therefore the hyperfine field of the Mn^{4+} ion is mainly composed of the Fermi-contact term, which is isotropic and oppositely directed to the magnetic moment of the ion and parallel to the electron spin **S**. Since the hyperfine interaction is rather effectively denoted as $A\mathbf{I}\cdot\mathbf{S}$ for the orbital singlet ion,[45] which corresponds to the Zeeman interaction of nuclear magnetic moment $\gamma\hbar\mathbf{I}$ subject to the Fermi-contact field $\mathbf{H}_F$, the hyperfine field is simply expressed to be

$$\mathbf{H}_N=\mathbf{H}_F=-(A/\gamma\hbar)\mathbf{S}, \quad (5)$$

where A is an isotropic hyperfine coupling constant. So the ^{55}Mn NMR frequency of the Mn^{4+} ions given by $\nu = \gamma H_N/2\pi h$ is proportional to $|\mathbf{S}|$ and its ^{55}Mn NMR spectra are expected to be a single line with narrow width. The relation between $\mathbf{H}_N$ and $\mathbf{S}$ together with magnetic moment $\mathbf{m}$ is shown in Fig. 4(c).

As for the hyperfine field for the Mn^{3+} ion ($3d^4$, ^5D) with a hole plus a half-filled shell, the situation is somewhat complicated owing to the orbital degeneracy in V_c.[45] The degeneracy of an orbital doublet E_g is removed to two orbital states denoted as A_{1g} and B_{1g} by the deformation of the crystal field to the tetragonal one caused mainly by the Jahn-Teller effect. The ground state B_{1g} is specified by the wave function $|X^2-Y^2\rangle$ when the tetragonal distortion is of a prolate type. In case an orthorhombic distortion is superposed the doublefold E_g states are not only split, but also admixed, so that the orbital ground state is of the form[45]

$$\psi_g = \cos\phi|X^2-Y^2\rangle + \sin\phi|3Z^2-r^2\rangle, \tag{6}$$

where $\cos\phi$ and $\sin\phi$ are normalization factors.

As given in Appendix A, the dipolar hyperfine field for the Mn^{3+} ion is calculated by using the ground-state wave function (6), and the result is $\mathbf{H}_d = \mathsf{D}\hat{\mathbf{e}}_\mathbf{m}$, where $\hat{\mathbf{e}}_\mathbf{m}$ is a unit vector of magnetization $\mathbf{m}$ of the Mn^{3+} ion and D is the dipolar hyperfine field coupling tensor. Therefore when the singlet ground state of the Mn^{3+} ion is specified by the wave function (6) the total hyperfine field is expressed as follows:[47]

$$\mathbf{H}_N = \mathbf{H}_F + \mathbf{H}_d = -|H_F|\hat{\mathbf{e}}_\mathbf{m} + \mathsf{D}\hat{\mathbf{e}}_\mathbf{m}. \tag{7}$$

It is noted that the orbital hyperfine field for the Mn^{3+} ion can be neglected here compared with the main terms, since H_1 is evaluated, using $\langle r^{-3}\rangle_{\text{a.u.}} = 4.79$ a.u. (Ref. 46) and $\Delta g \approx 0.01$ (Ref. 48) or 0.05 (Ref. 35), to be -6 or -30 kG, respectively. Then the total hyperfine field $\mathbf{H}_N$ is approximately in opposite direction to $\mathbf{m}$ and is directed against the local tetragonal axis δ with the following angle α (Ref. 49):

$$\tan\alpha = \frac{H_F - \frac{1}{2}H_d'}{H_F + H_d'}\tan\theta. \tag{8}$$

The relation between α and θ together with $\mathbf{m}$, $\mathbf{S}$, and $\mathbf{H}_N$ is shown in Fig. 4(c).

B. ^{55}Mn NMR frequency

In the analysis of the ^{55}Mn NMR frequency, it is convenient to use another reference frame xyz where the z axis is parallel to the direction of the magnetic moment of the ion in the Mn_{12} cluster, i.e., the c axis, and x axis is in the plane containing the z and Z axes as shown in Fig. 4(b), where θ is an angle between the magnetic moment and the Z axis. We assume $\eta = 0$; then, the hyperfine Hamiltonian is transformed as follows:

$$\begin{aligned}\langle\psi_g|\mathcal{H}_{\text{hyp}}|\psi_g\rangle &= -\gamma\hbar\mathbf{I}\cdot(\mathbf{H}_F+\mathbf{H}_d)\\ &\quad+\{e^2q_{ZZ}Q/4I(2I-1)\}[3I_z^2-I(I+1)]\\ &= -\gamma\hbar[H_F\cdot I_z-(1/2)(3\cos^2\theta-1)H_d'\cdot I_z\\ &\quad-(3/4)\sin 2\theta H_d'\cdot I_x]+e^2q_{ZZ}Q/\{4I(2I-1)\}\\ &\quad\times[(1/2)(3\cos^2\theta-1)\{3I_z^2-I(I+1)\}\\ &\quad+(3/2)\sin 2\theta(I_zI_x+I_xI_z)\\ &\quad+(3/2)\sin^2\theta(I_x^2-I_y^2)],\end{aligned} \tag{9}$$

where the off-diagonal terms of Zeeman and quadrupole terms are perturbations to their respective main terms.[47]

Taking into account the main term in Eq. (9), the NMR frequency ν_m corresponding to the transition $m-1\leftrightarrow m$ is given by

$$\begin{aligned}\nu_m &= |E_{m\_1}-E_m|/hH\\ &= \nu_F-(1/2)(3\cos^2\theta-1)\{\nu_d-(m-1/2)\nu_Q\}\\ &\quad+\text{higher-order terms},\end{aligned} \tag{10}$$

where ν_F and ν_d are obtained from the isotropic part of the hyperfine field H_F and the anisotropic one H_d', respectively, by the relation $\nu = \gamma|H|/2\pi h$ between frequency and field, and ν_Q is the quadrupole frequency $3e^2q_{zz}Q/\{2I(2I-1)h\}$. The higher-order terms, which are related to the off-diagonal term in Eq. (9), are less than a few percent compared with the main terms and can be neglected.

In the case of the Mn^{4+} ion the dipolar hyperfine field is zero; then, ν_m is simply to be

$$\nu_m = \nu_F + (1/2)(3\cos^2\theta-1)(m-1/2)\nu_Q. \tag{11}$$

When the external field $H(H \ll H_N)$ is applied along the c axis, then the NMR frequency can be approximated to vary as $\nu_m + \gamma H\cos\beta/2\pi h$, where β is the angle between $\mathbf{H}$ and $\mathbf{H}_N$.

Using Eq. (10), we can obtain the following expression of the resonance field H_{res} for the central NMR frequency $\nu_{-1/2\leftrightarrow 1/2} = \gamma H_{\text{res}}/2\pi h$:

$$H_{\text{res}} = H_F + (1/2)(3\cos^2\theta-1)H_d' = H_N(\theta); \tag{12}$$

therefore, we can analyze the resonance field H_{res} by means of separating the dipolar contribution in accordance with θ from the resonance frequency obtained.

IV. INTERPRETATION OF ^{55}Mn NMR AND DISCUSSION

A. Mn^{4+} ion

The hyperfine field of the Mn^{4+} ion deduced from the resonance frequency in Fig. 2 is 218.4 ± 0.1 kG, which is appreciably smaller as compared with both the theoretically calculated and the experimentally observed values as we see below in other oxides. Theoretically the Fermi-contact hyperfine field per unpaired d electron, which is defined by χ, was calculated by Freeman and Watson by summing up totally the polarized contribution of inner $1s$, $2s$, and $3s$ electrons for various valence states of free manganese ions.[46] The value of χ for Mn^{4+} is -2.34 a.u. Hence we find

$H_F(\mathrm{calc}) = 3\chi_{Mn^{4+}} = -293$ kG using the conversion factor 1 a.u. $= 4.17 \times 10$ kG for χ in atomic units.[45] The observed hyperfine field for Mn^{4+} ions in Mn_{12}Ac is smaller by 26% than the calculated value. Moreover, there is similar evidence for the reduction of the hyperfine fields in Mn^{4+} ions in an isomorphous Mn_{12} cluster, the preliminary measurements on the ^{55}Mn NMR in the Mn^{4+} ion in $[Mn_{12}O_{12}(O_2CPh)_{16}(H_2O)_4] \cdot 2PhCO_2H$ (Ref. 50) yield almost same resonance frequencies as the present case. On the contrary, in lithium manganese ferrite $Li_{0.5}Mn_{0.5}Fe_2O_4$, the hyperfine fields for ^{55}Mn nuclei in Mn^{4+} ions are observed to be -293.8 ± 0.1 kG.[51] The hyperfine field concerning Mn^{4+} ions in the paramagnetic state is reported to give $H_N = -301.86$ kG (for Mn^{4+} ions diluted in MgO) (Ref. 45) and -290.90 kG (for Mn^{4+} ions diluted in Al_2O_3) (Ref. 45). These experimental values for the hyperfine fields in Mn^{4+} ions are nearly the same as the above theoretical one. So we can imply that ^{55}Mn NMR associated with the Mn^{4+} ion in the Mn_{12} cluster is usually observed around 230 MHz ($H_N = -218$ kG), which corresponds to about 74% of the calculated value. The following fact should be noted: recent polarized-neutron-diffraction measurements on Mn_{12}Ac also indicate that the local magnetic moments for Mn(1) sites are reduced to $78 \pm 4\%$ of the full value of $3.0\mu_B$ for Mn^{4+} ions and those for Mn(2) [Mn(3)] sites to be $92 \pm 4\%$ [$94 \pm 3\%$] of the full value of $4.0\mu_B$ for Mn^{3+} ions.[34] The theoretical calculation of the electronic structure for the Mn_{12}Ac cluster based on the density functional formalism has presented a considerable amount of reduction for the local magnetic moments of manganese ions: $2.6\mu_B$ (86% of the full value $3.0\mu_B$) for Mn^{4+} ions and $3.6\mu_B$ (90% of the full value $4.0\mu_B$) for Mn^{3+} ions, respectively.[14] The reduction factor of 26% for Mn^{4+} ions observed in the present NMR measurement is consistent with that of the polarized-neutron-diffraction result. We believe a large amount of reduction of the Mn^{4+} hyperfine field obtained for Mn_{12}Ac by the present NMR measurement is related to the covalence and strong exchange coupling between Mn(1) and Mn(2) via oxygen ions as mentioned in Ref. 14.

Next, we interpret the ^{55}Mn NMR spectra of the inset of Fig. 3. As was previously noted, the spectra $\nu_\uparrow$ arise from the ^{55}Mn nuclei in Mn^{4+} ions belonging to clusters whose moments are parallel to the external field while those of $\nu_\downarrow$ arise from ones belonging to clusters whose moments are antiparallel to the external field. We find that the intensity of the spectra $\nu_\uparrow$ is always larger than that of $\nu_\downarrow$. This is due to the fact that the spin-echo decay time T_2 is longer for the $\nu_\uparrow$ line than that for $\nu_\downarrow$. As time passes, the spin-echo intensity of the $\nu_\uparrow$ line has a trend to increase, while that of $\nu_\downarrow$ line to decrease. This fact reflects the relaxation of cluster magnetization in the presence of an external field after ZFC; the increase of the intensity of the $\nu_\uparrow$ line accompanying the decrease of that of the $\nu_\downarrow$ line corresponds to the gradual change of the magnetization direction of the cluster from down to up with respect to the field direction during the time elapsed. The fact that the slope of the ν-H relation coincides with the value of $^{55}\gamma/2\pi$ means that the hyperfine field of the Mn^{4+} ion is just parallel to the external field and its own local moment.

We mention here the small quadrupole splitting $\Delta\nu_Q = 0.72 \pm 0.05$ MHz. From the local symmetry of the Mn(1) site in Mn_{12}Ac molecules,[7] each Mn^{4+} ion is subject to an octahedral crystal field with an axial-symmetry axis which is parallel to the c axis. The electric-field gradient V_{ZZ} at ^{55}Mn nuclei in Mn^{4+} ions originates solely from octahedrally surrounding O^{2-} ions with symmetry lower than the cubic one.[7] There may be a second-order contribution to the quadrupole coupling that is due to the distortion of the spherical electron shells of Mn^{4+} ions induced by the external charges, and the induced gradient is given to be $-\gamma_\infty V_{ZZ}$ in which γ_∞ is an antishielding factor. Then the total electric-field gradient is to be $q_c = (1-\gamma_\infty)V_{ZZ}$.[46] From the value of $\Delta\nu_Q = 3e^2q_cQ/\{2I(2I-1)h\} = 0.72 \pm 0.05$ MHz, we find $e^2q_cQ/h = 4.80 \pm 0.33$ MHz.

B. Mn^{3+} ion

Since an orbital doublet ion such as the Mn^{3+} ion is stabilized in energy by lowering the symmetry of ligands to remove the degeneracy in the cubic symmetry, the ground-state wave function becomes asymmetric, which gives rise to a considerable amount of the dipolar hyperfine field on a nuclear site. In fact, as for the Mn^{3+} ions both at Mn(2) and at Mn(3) sites, the octahedral ligands composed of oxygens are of tetragonal symmetry in the first approximation and in addition have lower symmetry than the tetragonal one. As shown in Fig. 1(b), the Mn^{3+} ion at the Mn(2) site has mainly tetragonal symmetry (elongated) with the axially symmetric axis δ, which lies in the direction of 11.7° from the c axis. On the other hand, the Mn^{3+} ion at the Mn(3) site has a considerable rhombic component[7] in addition to the tetragonal one, in which the δ axis makes an angle of 36.2° from the c axis.

As already noted, the hyperfine field of the Mn^{3+} ion has an anisotropic dipolar term H_d besides an isotropic Fermi-contact term H_F. As is clear from Eq. (10), the ^{55}Mn NMR frequency for the Mn^{3+} ion varies appreciably depending on the two frequencies ν_F and ν_d and an angle θ shown in both Figs. 1(b) and 4(c). We next evaluate the two parameters H_F and H_d', of the hyperfine field. The value of χ calculated for the free Mn^{3+} ion is given to be -2.91 a.u.,[46] which corresponds to $4\chi_{Mn^{3+}} = -485$ kG$\equiv H_F$(calc) for the calculated value of Fermi-contact term in the Mn^{3+} ion. On the other hand, the dipolar hyperfine field parameter in Eq. (A3) is given to be $h_d = (4/7)\mu_B\langle r^{-3}\rangle = (2/7) \times 125\langle r^{-3}\rangle_{\mathrm{a.u.}}$ (Ref. 45) $= +171$ kG$\equiv h_d$(calc), using $\langle r^{-3}\rangle = 4.79$ a.u. for the free Mn^{3+} ion.[46]

However, it turns out that the use of these theoretical values fails to explain our NMR results. Then in order to obtain reasonable agreement between the experiment and calculation it is necessary to take into account the reduction factor for the Fermi-contact and dipolar hyperfine fields. Here, as for the dipolar hyperfine field, we apply the reduction factor for $3d$-electron spins obtained by neutron-diffraction measurements because the dipolar hyperfine field is directly related to the local moment of the ion. Using the experimental value of the Mn^{3+} magnetic moment, $3.69 \pm 0.04\mu_B$ ($8 \pm 1\%$ reduced from $4.0\mu_B$) at Mn(2), which was obtained by

TABLE I. Hyperfine field of the Mn^{3+} ion in $Mn_{12}Ac$ is interpreted to follow the expression $H_N(\theta)=H_F+(1/2)(3\cos^2\theta-1)H_d'$ by adopting relevant values of H_F and H_d' and by putting a fixed value into the angle θ, suitable for the Mn(2) ($\theta=11.7°$) or Mn(3) ($\theta=36.2°$) site. The effective dipolar hyperfine field parameter $H_d'=h_d\cos 2\phi$ can be obtained by using the ground-state wave function $\psi_g=\cos\phi|X^2-Y^2\rangle+\sin\phi|3Z^2-r^2\rangle$ with admixing coefficients $\cos\phi$ and $\sin\phi$. Here we adopted the value of the Fermi-contact hyperfine field $H_F=-412.4$ kG and that of dipolar hyperfine field parameter $h_d=\frac{4}{7}\mu_B\langle r^{-3}\rangle=+157.3$ kG, which is reduced by 8% from the calculated value $h_d(\text{calc})=+171$ kG for free Mn^{3+} ions taking into account the value of the Mn(2) moment determined by neutron diffraction measurements in Ref. 34. The calculated values for the hyperfine fields are from Ref. 46.

	Fermi-contact term (kG)	Dipolar term (kG)
Free Mn^{3+} ion (calc)	$H_F(\text{calc})=-485$	$h_d(\text{calc})=+171$
8% reduced for h_d		$h_d=0.92\times h_d(\text{calc})=+157.3$
Mn^{3+} ion in $Mn^{12}Ac$	$H_F=-412.4$	$H_d'=h_d\cos 2\phi$
Mn(2) ($\theta=11.7°$)	-412.4	$+157.3$ ($\phi=0.0°$)
Mn(3) ($\theta=36.2°$)	-412.4	$+140.5$ ($\phi=13.4°$)
$H_N=H_F+\frac{1}{2}(3\cos^2\theta-1)H_d'$		

the polarized-neutron-diffraction measurement,[34] we can estimate the dipolar hyperfine field parameter to be $h_d=h_d(\text{calc})\times 0.92=+157.3$ kG for the Mn^{3+} ion at Mn(2). Next, we take $H_d'=h_d$ by assuming the tetragonal symmetry of sixfold O^{2-} ligands around the Mn^{3+} ion at Mn(2) without any other lower symmetry. In order to obtain the experimental value $H_N=-264.8$ kG from Eq. (12) by using the values $H_d'=+157.3$ kG and $\theta=11.7°$, it is necessary to choose the Fermi-contact hyperfine field to be $H_F=-412.4$ kG for the Mn^{3+} ion at Mn(2). This value corresponds to 85% of the above-calculated value of -485 kOe. These values of the hyperfine fields, $H_F=-412.4$ kG and $H_d'=+157.3$ kG, are comparable to $H_F=-414.8$ kG and $H_d'=+113.6$ kG deduced from ESR measurements for the Mn^{3+} ion in TiO_2.[48]

Since it is clear in general that H_F is roughly constant for ions of common valence in common environments,[46] we here reasonably apply the same value of H_F to the Mn^{3+} ion at the Mn(3) site. Then by substituting the observed value of $H_N=-345.4$ kG, $H_F=-412.4$ kG, and $\theta=36.2°$ in Eq. (12) we find $H_d'=+140.5$ kG for the Mn^{3+} ion at the Mn(3) site. As shown in Eq. (A3), the effective dipolar hyperfine field parameter $H_d'=h_d\cos 2\phi$ in dipolar hyperfine coupling tensor D varies depending on the ratio of admixing of the $|3Z^2-r^2\rangle$ wave function to $|X^2-Y^2\rangle$ as specified by Eq. (6). The obtained result $H_d'=+140.5$ kG for Mn(3) can be reasonably interpreted taking into account admixing coefficients for the ground-state wave function, $\cos\phi$ and $\sin\phi$, to satisfy the relation $\cos 2\phi=0.893$ ($\phi=13.4°$). The quantitative interpretation of hyperfine fields for the Mn^{3+} ions in $Mn_{12}Ac$ is arranged in Table I. For the case of the Mn^{3+} ion at the Mn(3) site the ground-state wave function has to be

TABLE II. Summary of ^{55}Mn NMR results for $Mn_{12}Ac$: ^{55}Mn NMR frequencies, quadrupole-coupling constants, hyperfine fields, hyperfine coupling constants, and tetragonal ratio of octahedral environments around the Mn^{3+} ion.

Site valence	Mn(1) Mn^{4+}	Mn(2) Mn^{3+}	Mn(3) Mn^{3+}
ν (MHz)	230.2 ± 0.1	279.4 ± 0.1	364.4 ± 0.1
$\Delta\nu_Q$ (MHz)	0.72 ± 0.05	4.3 ± 0.1	2.9 ± 0.1
e^2qQ/h (MHz)	4.80 ± 0.33	30.6 ± 0.7	40.6 ± 1.5
H_N (kOe)	-218.2 ± 0.1	-264.8 ± 0.1	-345.4 ± 0.1
H_F (kOe)	-218.2 ± 0.1	-412.4	-412.4
H_d' (kOe)		$+157.3$	$+140.5$
$\theta=\delta\wedge c$		11.7°	36.2°
$\alpha=\delta\wedge H_N$		21.7°	52.4°
$\cos(\alpha-\theta)$		0.98	0.96
A_z (MHz)	153.5	139.7	182.2
Tetragonal ratio		1.16	1.11

defined under the influence of a considerable rhombic component of the crystal field, which results in a smaller dipolar hyperfine field than that for Mn(2) in terms of the admixing coefficient $\cos 2\phi$. The quadruple coupling constant $e^2q_{ZZ}Q/h$ can be deduced from $\Delta\nu_Q=4.3\pm0.1$ for ^{55}Mn at Mn(2) and 2.9 ± 0.1 MHz for ^{55}Mn at Mn(3) to be 30.6 ± 0.7 MHz and 40.6 ± 1.5 MHz, respectively.

We have analyzed the hyperfine fields of Mn^{4+} and Mn^{3+} ions in $Mn_{12}Ac$ and quantitatively clarified that the former only has an isotropic term H_F, while the latter has an anisotropic term H_d in addition to H_F. Using these parameters we can deduce total angular dependence of the hyperfine fields for Mn^{3+} ions as expressed in Eq. (7). The obtained results from the present NMR studies are summarized in Table II. For the case of Mn^{3+} ions [both Mn(2) and Mn(3)] the total hyperfine fields $\mathbf{H}_N$ are not parallel to their own spins except for $\theta=0$ and $\pi/2$, as noted in Eq. (8), but make an angle $\alpha-\theta$ from the c axis, which causes the ^{55}Mn NMR frequency $\nu_{-1/2\leftrightarrow1/2}={}^{55}\gamma|\mathbf{H}_N+\mathbf{H}|/2\pi$ in the external field approximately to be $\{{}^{55}\gamma H_N\pm{}^{55}\gamma\cos(\alpha-\theta)H\}/2\pi$ in the condition of $H\ll H_N$. Therefore the effective value of $\gamma/2\pi$, $\gamma_{\text{eff}}/2\pi$, obtained from the frequency-field diagrams for Mn^{3+} ions in Fig. 3 is expected to be $({}^{55}\gamma/2\pi)\cos(\alpha-\theta)$. The fact that the value $\cos(\alpha-\theta)$ evaluated from the values of θ and α in Table II deviates less than 0.04 from 1 implies that the value of $\gamma_{\text{eff}}/2\pi$ for ^{55}MN NMR in Mn^{3+} ions would be quite similar to that of ${}^{55}\gamma/2\pi$ of the free ^{55}Mn nucleus. This is the case just observed in Fig. 3 for ^{55}Mn NMR in both Mn^{3+} ions.

Quite recently, Furukawa *et al.*[52] presented a report on the zero-field ^{55}Mn NMR and field dependence of the NMR frequencies for the oriented powder $Mn_{12}Ac$, together with the nuclear relaxation rate $1/T_1$. They discussed nuclear relaxation by thermal fluctuations in the $S=10$ spin states, and from the frequency-field diagram they denoted the standard picture of magnetic structure in the cluster. They assumed that the dominant part of the hyperfine field of the ^{55}Mn nuclei in the Mn^{3+} ion was the core-polarization term, ne-

glecting dipolar terms. Accordingly, the identification of the two spectra concerned with Mn(2) and Mn(3) remains unsolved. Here we have reasonably identified these two spectra around 280 and 364 MHz by taking into account the contribution from the dipolar hyperfine field to be due to Mn^{3+} ions at Mn(2) and the ones at Mn(3), respectively.

C. Hyperfine interaction in the Mn_{12}Ac cluster

We discuss here the total hyperfine interaction between manganese nuclei and the molecular spin $S=10$ in Mn_{12}Ac by taking into account three kinds of hyperfine coupling constants obtained for Mn(1), Mn(2), and Mn(3), respectively. The roles of the hyperfine interaction in the magnetic relaxation of Mn_{12}Ac clusters have been discussed by several authors.[6,10–13,16] The hyperfine interactions concerned with eight Mn^{3+} and four Mn^{4+} ions in the Mn_{12}Ac cluster have been studied quantitatively by Hartmann-Boutron *et al.*[2] assuming two kinds of hyperfine coupling constants for manganese ions. Since the present ^{55}Mn NMR results in Mn_{12}Ac show us three kinds of ground states for manganese ions in the cluster, we express the total magnetic hyperfine interaction in the Mn_{12} cluster in terms of three kinds of hyperfine tensors[45] A_{xyz} for single ions as

$$\langle \mathcal{H}_n^{\rm tot}\rangle = \sum_{r=1}^{12} \langle \mathcal{H}_n\rangle_r = \sum_{i=1}^{4} \mathbf{S}_i^{(1)}\mathsf{A}_i^{(1)}\mathbf{I}_i^{(1)} + \sum_{j=1}^{4} \mathbf{S}_j^{(2)}\mathsf{A}_j^{(2)}\mathbf{I}_j^{(2)} + \sum_{k=1}^{4} \mathbf{S}_k^{(3)}\mathsf{A}_k^{(3)}\mathbf{I}_k^{(3)}, \quad (13)$$

where the superscripts (1), (2), and (3) are concerned with Mn(1), Mn(2), and Mn(3) sites, respectively. Each sum is limited over manganese ions within one of the Mn(1), Mn(2), and Mn(3) sites. Next, we take into account the ferrimagnetic structure in the Mn_{12} cluster where the quantization axis is taken to be as the z axis along the c axis and assuming in the ground state that the x and y components of the electron spin are replaced by 0. Then Eq. (13) can be simplified to be

$$\begin{aligned}\langle \mathcal{H}_n^{\rm tot}\rangle_{\rm ferri} &= S_z^{(1)}\mathsf{A}_{zz}^{(1)}\sum_{i=1}^{4} I_{zi}^{(1)} + S_z^{(2)}A_{zz}^{(2)}\sum_{j=1}^{4} I_{zj}^{(2)} + S_z^{(3)}A_{zz}^{(3)}\sum_{k=1}^{4} I_{zk}^{(3)} \\ &= +\frac{3}{2}\mathsf{A}_{zz}^{(1)}\sum_{i=1}^{4} I_{zi}^{(1)} - 2\mathsf{A}_{zz}^{(2)}\sum_{j=1}^{4} I_{zj}^{(2)} - 2\mathsf{A}_{zz}^{(3)}\sum_{k=1}^{4} I_{zk}^{(3)}. \end{aligned} \quad (14)$$

By use of the relation $\nu = A_{zz}\cdot S/h$ from the observed central frequencies $\nu^{(1)}=230$ MHz, $\nu^{(2)}=280$ MHz, and $\nu^{(3)}=365$ MHz, we can deduce the hyperfine coupling constants divided by h, referring to $\mathsf{A}_{zz}^{(1)}/h$, $\mathsf{A}_{zz}^{(2)}/h$, and $\mathsf{A}_{zz}^{(3)}/h$ as $\mathsf{A}_z^{(1)}$, $\mathsf{A}_z^{(2)}$, and $\mathsf{A}_z^{(3)}$ to be 153.5, 139.7, and 182.2 MHz, respectively. Accordingly for the total hyperfine interaction in the Mn_{12}Ac molecule at the ferrimagnetic ground state, we obtain the following equation in MHz:

$$\left(\frac{1}{h}\right)\langle \mathcal{H}_n^{\rm tot}\rangle_{\rm ferri} = +\frac{3}{2}(153.5)\sum_{i=1}^{4} I_{zi}^{(1)} - 2(139.7)\sum_{j=1}^{4} I_{zj}^{(2)} - 2(182.2)\sum_{k=1}^{4} I_{zk}^{(3)}. \quad (15)$$

Every sum takes integer values from -10 to 10 considering $I(^{55}\mathrm{Mn})=\frac{5}{2}$. The number of allowed values of the energy is $(2\times 10+1)^3=9261$.

The maximum value of the effective hyperfine interaction for ferrimagnetic coupling in the Mn_{12}Ac molecule can be obtained from the next relation

$$\left(\frac{1}{h}\right)\langle \mathcal{H}_n^{\rm tot}\rangle_{\rm ferri} = 2\times 10\left(\frac{3}{4}\times 153.3 + 139.7 + 18.2\right)\ \mathrm{MHz} = 0.29\ \mathrm{cm}^{-1}. \quad (16)$$

From the definition $\langle \mathcal{H}_n^{\rm tot}\rangle_{\rm ferri} = g_z\mu_B S_z\cdot h_e$ we can estimate the maximum nuclear hyperfine field $h_e=324$ G, using $g_z=1.93$,[35] which is seen by the total spin $S=10$. This value amounts to 2.5 times as large as the nuclear hyperfine field for a single Mn^{4+} ion (137 G) in Mn_{12}Ac. Therefore every electronic energy level for the state $|S,m\rangle$ determined by Eq. (1) is inhomogeneously broadened through a hyperfine interaction with 12 ^{55}Mn nuclei into 21^3 sublevels with total spread of about 0.3 cm^{-1} (0.42 K). The broadened energy levels which approximately appear like a continuum are symbolically depicted in Ref. 2. This amount of hyperfine interaction was also confirmed by measurements of the magnetic specific heat at low temperatures where an appreciable nuclear contribution appeared below 0.5 K in Mn_{12}Ac.[28,30]

Next, we refer to the other components of the hyperfine coupling tensor $\mathsf{A}_{xyz}^{(p)}/h$ in MHz which play an important role in the magnetization relaxation and also in the ^{55}Mn nuclear relaxation in Mn_{12}Ac. For Mn(1) the hyperfine interaction is isotropic; then, $\mathsf{A}_{xyz}^{(1)}/h$ is $153\times\mathbf{1}$ MHz where $\mathbf{1}$ is a unit tensor. The hyperfine coupling tensors $\mathsf{A}_{xyz}^{(2)}/h$ for Mn(2) and $\mathsf{A}_{xyz}^{(3)}/h$ for Mn(3) are given in Appendix B. By applying these values to Eq. (13) we can represent the total hyperfine interaction in the cluster. This type of total hyperfine interaction in the Mn_{12} cluster is understood to be strictly anisotropic in character.

The above transverse component of the hyperfine interaction would contribute in the magnetic relaxation[2,6,12] of the cluster to promoting both the transition between $|S,m\rangle$ levels and quantum tunneling as well as the molecular-dipole interaction and higher-order crystal anisotropy. Luis, Baltolome, and Fernandez[13] calculated the relaxation rate as a function of the longitudinal magnetic field, taking into account dipolar fields among clusters together with hyperfine fields and the quartic magnetic anisotropy, and explained the nonlinear spin relaxation rate in terms of spin-phonon-induced tunneling depending on the longitudinal external field. On the other hand, Leuenberger and Loss,[15] neglecting the hyperfine and dipolar fields for $T>1$ K, calculated the relaxation rate as a

function of the longitudinal magnetic field based on phonon-assisted spin tunneling induced by the quartic magnetic anisotropy and weak transverse magnetic fields. Their result was also in good agreement with experimental relaxation rates including all resonance peaks. It has been assured from these theoretical calculations that any extent of a transverse component is essential to explain the magnetic relaxation in Mn_{12} clusters, no matter what the phonon-assisted quantum transition may be induced by an external or internal origin.

D. Relaxation of Mn_{12}Ac cluster magnetization

It is noted that in the present relaxation experiment at 2.0 K the square-root decay of magnetization, typically shown in Fig. 5 for external magnetic fields of 1.2 and 1.4 T, has been observed in nearly the whole range between 0.200 and 1.900 T in short times. In the inset of Fig. 5 the gradual decrease of τ versus H can be interpreted as the relaxation governed by the spin-phonon interaction[2,8] due to the decrease of the potential barrier. The occurrence of regular minima of τ at every 0.45 T, which is nearly equal to $D/g\mu_B$ ($\equiv H_1$) using $D \approx 0.58$ K, implies that resonant quantum tunneling[19,20] arises between the levels of the two wells having the same energy. This feature is found obviously above 2.0 K, while such a marked behavior below 1.8 K cannot be clearly observed. Taking into account such a thermal effect—that the relaxation times depend strongly on temperatures—we understood that the appearance of dips corresponds to phonon-assisted resonant quantum tunneling which has been suggested[39,40] and discussed[19,20] by several authors.

It is well known that the recovery curve of the cluster magnetization M is expressed by a stretched-exponential function $M = M_0[1 - \exp\{-(t/\tau)^{\beta}\}]$ after reversal of the field or $M = M_0 \exp\{-(t/\tau)^{\beta}\}$ in zero field.[53] It has been found in zero-field relaxation for Mn_{12}Ac that the exponent β is strongly temperature dependent: below 2.0 K, β is close to 0.5 and increases linearly with temperature up to 2.4 K to reach $\beta = 1.1$, then slightly decreasing at higher temperatures and long times to be $\beta = 1$.[22] Theoretically, it was shown that in zero field at very low temperature, where pure quantum tunneling between the ground states ($m = \pm 10$) occurs, $\beta = 1/2$ holds in short times while $\beta = 1$ in long times.[10,11] Evidence of a square-root t relaxation in short times has been observed for Fe_8 below 0.4 K in low fields (0–20 mT) (Ref. 53) and also for Mn_{12}Ac at 0.9 K in 4.02 T.[26]

The relaxation time of the magnetization in Mn_{12}Ac, investigated in long times by the use of proton NMR by Jang *et al.*[38] has been measured as a function of longitudinal magnetic field at 2.4 K. Their result was interpreted as the background relaxation of the Arrhenius law due to thermal excitations accompanying relaxation minima at level crossings. However, in our case the result of the relaxation time shown in the inset to Fig. 5 indicates that the background relaxation does not follow strictly the Arrhenius law, showing a more abrupt decrease with external field. The background relaxation based on the thermal excitation over the barrier is expected to be represented by an exponential law $\tau = \tau_0 \exp\{(\Delta - g_z\mu_B S_z H)/kT\}$ with $g_z = 1.93$,[35] $S = 10$, and $\tau_0 = 8 \times 10^{-7}$ s,[38] which is shown in the inset to Fig. 5 by the dotted line for comparison. Such a deviation may be probably due to the relaxation times obtained in short times, the reason for which has been studied now.

The above two facts—the square-root t relaxation in short times and the deviation of the relaxation time from the Arrhenius law—are probably relevant to the present experimental situation—measurements at 2.0 K in a field of about 1 T—which is effectively compared to the phonon-assisted tunneling regime.[54]

V. CONCLUSION

By an analysis of the hyperfine fields of ^{55}Mn nuclei associated with Mn^{3+} and Mn^{4+} ions, we have interpreted three kinds of ^{55}Mn NMR composed of fivefold quadrupole-split lines and identified them to the corresponding sites in Mn_{12}Ac clusters. Namely, the central frequencies 230.2 $\pm$ 0.1 MHz, 279.4 $\pm$ 0.1 MHz, and 364.4 $\pm$ 0.1 MHz were assigned to be ^{55}Mn NMR originating in Mn^{4+} ions at Mn(1) sites, Mn^{3+} ions at Mn(2) sites, and Mn^{3+} ions at Mn(3) sites in Mn_{12}Ac molecules, respectively.

In Mn_{12}Ac crystal the hyperfine field concerned with the Mn^{4+} ion has been found to be largely reduced to 74% compared with the calculated value and the ones in other compounds. The hyperfine field of the Mn^{4+} ion, which is mainly due to the Fermi-contact term, is isotropic, while that of Mn^{3+} is anisotropic. The hyperfine field of the Mn^{3+} ion demonstrates the contribution of the appreciable dipolar term, which is deduced from the admixed wave function relevant to the low symmetry of the crystal field, to the total hyperfine field. The magnitude of the total hyperfine interaction in the Mn_{12} cluster at the ferromagnetic ground state is estimated to be 0.3 cm^{-1} at most using 12 hyperfine constants of the single manganese ion obtained from present NMR results. Therefore the exact energy levels which are specified by $|S,m\rangle$ and determined by the spin Hamiltonian (1) are broadened like a continuum with a half width of 0.3 cm^{-1} owing to the hyperfine interaction. The amount of the above hyperfine interaction corresponds to the nuclear hyperfine field $h_e = 0.32$ kG acting on Mn_{12} cluster spin. The total hyperfine coupling tensor for the Mn_{12} cluster has been obtained by summing up 12 hyperfine coupling tensors of single ions that are composed of both isotropic (Mn^{4+}) and anisotropic (Mn^{3+}) components.

As for magnetic relaxation in Mn_{12}Ac in a longitudinal field, the cluster magnetization relaxes nonexponentially in short times; i.e., it shows a square-root t recovery curve at 2.0 K. The fact that the longitudinal-field dependence of the relaxation time in short times shows significant dips of more than one order of magnitude at every 0.45 T-step at 2.0 K demonstrates that the thermally assisted resonant quantum tunneling is active in the early stage of the magnetic relaxation at 2.0 K. By using ^{55}Mn NMR the magnetization relaxation in the fields can be measured in a few seconds after the reversal of the applied field. Measurements of the relaxation rates which increase significantly with application of measurable transverse applied fields are now in progress.

ACKNOWLEDGMENTS

We thank B. Barbara for fruitful discussions. We thank also S. Miyashita and M. Chiba for continual interest and comments. Thanks are due to B. Imanari for assistance in final stage of this work. Finally, we thank F. Borsa and Y. Furukawa for showing a manuscript prior to publication. The present work was supported by a Grant-in-Aid for Scientific Research from Ministry of Education, Culture, Sports, Science and Technology of Japan.

APPENDIX A: DIPOLAR HYPERFINE FIELD

In order to calculate the dipolar hyperfine field for the Mn^{3+} ion, we adopt the expression of the nuclear dipole interaction with $3d$ electrons given in Ref. 45 for a dipolar hyperfine Hamiltonian and average it with respect to the ground-state wave function (6) as follows with only diagonal terms in notation of the *XYZ* frame remaining:

$$\mathcal{H}_d = -\frac{2\gamma\hbar\mu_B}{r^3}\xi\Bigg[\{L(L+1)-3L_Z^2\}\Bigg(S_Z I_Z - \frac{1}{2}S_X I_X - \frac{1}{2}S_Y I_Y\Bigg) - \frac{3}{2}iL_Z(S_X I_Y - S_Y I_X]. \tag{A1}$$

Then the effective dipolar hyperfine interaction can be obtained, using $\xi = -1/42$ for $S=2$ and $L=2$,[45]

$$\langle\psi_g|\mathcal{H}_d|\psi_g\rangle = \cos 2\phi\,\frac{2\gamma\hbar\mu_B}{7}\langle r^{-3}\rangle \times\Bigg(S_Z I_Z - \frac{1}{2}S_X I_X - \frac{1}{2}S_Y I_Y\Bigg). \tag{A2}$$

By equating Eq. (A2) to the expression $-\gamma\hbar\mathbf{I}\cdot\mathbf{H}_d$, we get the dipolar hyperfine field for the present case, in terms of a unit vector $\hat{\mathbf{e}}_\mathbf{m}$ of the magnetization $\mathbf{m}$ of the Mn^{3+} ion:

$$\mathbf{H}_d = D\hat{\mathbf{e}}_m, \tag{A3}$$

where

$$D = H_d'\begin{pmatrix} -\frac{1}{2} & 0 & 0 \\ 0 & -\frac{1}{2} & 0 \\ 0 & 0 & 1 \end{pmatrix},$$

in terms of an effective dipolar hyperfine field parameter $H_d' = h_d\cos 2\phi$ with a parameter $h_d = (4\mu_B/7)\langle r^{-3}\rangle$.[47]

APPENDIX B: HYPERFINE COUPLING TENSOR FOR THE Mn^{3+} ION

The magnetic hyperfine interaction for the Mn^{3+} ion is expressed in the *XYZ* frame as follows[45,47]:

$$\langle\psi_g|\mathcal{H}_n|\psi_g\rangle = \mathbf{S}\cdot\mathsf{A}_{XYZ}\cdot\mathbf{I}, \tag{B1}$$

with

$$\mathsf{A}_{XYZ} = \tfrac{1}{2}\gamma\hbar|H_F|\mathbf{1} - \tfrac{1}{2}\gamma\hbar D. \tag{B2}$$

This relation is analogous to Eq. (7).

However, since in the Mn_{12}Ac cluster the quantization axis of spins should be defined along the crystal *c* axis, we express the above hyperfine coupling tensor in the *xyz* frame where the *z* axis is taken as the *c* axis. The result of the notation of the hyperfine coupling tensor transformed from the *XYZ* frame to the *xyz* frame in Fig. 4(b) is the following:

$$\langle\psi_g|\mathcal{H}_n|\psi_g\rangle = \mathbf{S}\cdot\mathsf{A}_{xyz}\cdot\mathbf{I}, \tag{B3}$$

with

$$A_{xyz} = \tfrac{1}{2}\gamma\hbar|H_F|\mathbf{1} - \frac{1}{2}\gamma\hbar D', \tag{B4}$$

where

$$D' = H_d'\begin{pmatrix} \frac{2-3\cos^2\theta}{2} & 0 & -\frac{3}{4}\sin 2\theta \\ 0 & -\frac{1}{2} & 0 \\ -\frac{3}{4}\sin 2\theta & 0 & \frac{3\cos^2\theta-1}{2} \end{pmatrix}. \tag{B5}$$

Accordingly, we get

$$\mathsf{A}_{xyz} = \frac{1}{2}\gamma\hbar|H_F|\begin{pmatrix} 1-\frac{2-3\cos^2\theta}{2}k & 0 & -\frac{3}{4}\sin 2\theta\cdot k \\ 0 & 1-\frac{1}{2}k & 0 \\ -\frac{3}{4}\sin 2\theta\cdot k & 0 & 1-\frac{3\cos^2\theta-1}{2}k \end{pmatrix}, \tag{B6}$$

with $k=H'_d/|H_F|$.

Then, using suitable values of θ, H_F, and H'_d in Table II, the hyperfine coupling tensors $\mathsf{A}^{(2)}_{xyz}$ for Mn(2) and $\mathsf{A}^{(3)}_{xyz}$ for Mn(3) are obtained in MHz as follows:

$$\mathsf{A}^{(2)}_{xyz}=\begin{pmatrix} 253.9 & 0 & -24.7 \\ 0 & 176.1 & 0 \\ -24.7 & 0 & 139.7 \end{pmatrix} \tag{B7}$$

and

$$\mathsf{A}^{(3)}_{xyz}=\begin{pmatrix} 221.0 & 0 & -53.0 \\ 0 & 180.5 & 0 \\ -53.0 & 0 & 182.2 \end{pmatrix}, \tag{B8}$$

respectively.

*Corresponding author. Electronic address: kubotk@nara-edu.ac.jp

[1] *Quantum Tunneling of Magnetization*, edited by L. Gunter and B. Barbara (Kluwer, Dordrecht, 1995).

[2] F. Hartman-Boutron, P. Politi, and J. Villain, Int. J. Mod. Phys. B **21**, 2577 (1996).

[3] I. Tupitsyn, N. V. Prokof'ev, and P. C. E. Stamp, Int. J. Mod. Phys. B **11**, 2901 (1997).

[4] E. M. Chudnovsky and J. Tejada, *Macroscopic Quantum Tunneling of Magnetic Moment* (Cambridge University Press, Cambridge, England 1997).

[5] A. Barbara, L. Thomas, F. Lionti, A. Sulpice, and A. Caneschi, J. Magn. Magn. Mater. **177–181**, 1324 (1998).

[6] B. Barbara, L. Thomas, F. Lionti, I. Chiorescu, and A. Sulpice, J. Magn. Magn. Mater. **200**, 168 (1999).

[7] T. Lis, Acta Crystallogr., Sect. B: Struct. Crystallogr. Cryst. Chem. **B36**, 2042 (1980).

[8] J. Villain, F. Hartman-Boutron, R. Sessoli, and A. Rettori, Europhys. Lett. **27**, 159 (1994).

[9] P. C. E. Stamp, Nature (London) **383**, 125 (1996); L. Gunther, Europhys. Lett. **39**, 1 (1997); A. Fort, A. Rettori, J. Villain, D. Getteschi, and R. Sessoli, Phys. Rev. Lett. **80**, 612 (1998); D. A. Garanin, X. M. Hidalgo, and E. M. Chudnovsky, Phys. Rev. B **57**, 13 639 (1998); Z. Zeng, D. Guenzburger, and D. E. Ellis, *ibid.* **59**, 6927 (1999); M. N. Leuenberger and D. Loss, *ibid.* **63**, 054414 (2001).

[10] N. V. Prokof'ev and P. C. E. Stamp, Phys. Rev. Lett. **80**, 5794 (1998).

[11] N. V. Prokof'ev and P. C. E. Stamp, J. Low Temp. Phys. **113**, 1147 (1998).

[12] D. A. Garanin, E. M. Chudnovsky, and R. Schilling, Phys. Rev. B **61**, 12 204 (2000).

[13] F. Luis, J. Bartolome, and J. F. Fernandez, Phys. Rev. B **57**, 505 (1998).

[14] M. R. Pederson and S. N. Khanna, Phys. Rev. B **60**, 9566 (1999).

[15] M. N. Leuenberger and D. Loss, Phys. Rev. B **61**, 1286 (2000).

[16] T. Pohjola and H. Schoeller, Phys. Rev. B **62**, 15 026 (2000).

[17] A. Caneschi, D. Gatteschi, R. Sessoli, A.-L. Barra, L.-D. Brunel, and M. Guillot, J. Am. Chem. Soc. **113**, 5873 (1991).

[18] R. Sessoli, H. L. Tsai, A. R. Schake, S. Wang, J. B. Vincent, K. Folting, D. Getteschi, G. Christon, and D. N. Hendrickson, J. Am. Chem. Soc. **115**, 1804 (1993).

[19] J. R. Friedman, M. P. Sarachik, J. Tejada, and R. Ziolo, Phys. Rev. Lett. **76**, 3830 (1996).

[20] L. Thomas, F. Lionti, R. Ballou, D. Gatteschi, R. Sessoli, and B. Barbara, Nature (London) **383**, 145 (1996).

[21] J. M. Hernandez, X. X. Zhang, F. Luis, J. Tejada, J. R. Friedman, and M. P. Sarachik, Phys. Rev. B **55**, 5858 (1997); J. A. A. J. Parenboom, J. S. Brooks, S. Hill, T. Hathaway, and N. S. Dalal, *ibid.* **58**, 330 (1998).

[22] L. Thomas, A. Caneschi, and B. Barbara, Phys. Rev. Lett. **83**, 2398 (1999).

[23] E. d. Barco, J. M. Hernandez, M. Sales, J. Tejada, H. Rakoto, J. M. Broto, and E. M. Chudnovsky, Phys. Rev. B **60**, 11 898 (1999).

[24] L. Bockacheva, A. D. Kent, and M. Walters, Phys. Rev. Lett. **85**, 4803 (2000).

[25] Y. Zhong, M. P. Sarachik, J. Yoo, and D. N. Hendrickson, Phys. Rev. B **62**, 9256 (2000).

[26] I. Chiorescu, R. Giraud, A. G. M. Jansen, A. Caneschi, and B. Barabara, Phys. Rev. Lett. **85**, 4807 (2000).

[27] F. Luis, J. Bartolome, J. F. Fernandez, J. Tejada, J. M. Hernandez, X. X. Zhang, and R. Ziolo, Phys. Rev. B **55**, 11 448 (1997); G. Bellessa, N. Vernier, B. Barbara, and D. Gatteschi, Phys. Rev. Lett. **83**, 416 (1999).

[28] M. A. Novak, A. M. Gomes, and R. E. Rapp, J. Appl. Phys. **83**, 6943 (1998).

[29] F. Fominaya, J. Vittain, P. Gandit, J. Chaussy, and A. Caneschi, Phys. Rev. Lett. **79**, 1126 (1997); M. Gomes, M. A. Novak, R. Sessoli, A. Caneschi, and D. Gatteschi, Phys. Rev. B **57**, 5021 (1998); M. Sales, J. M. Hernandez, J. Tejada, and J. L. Martinez, *ibid.* **60**, 14557 (1999).

[30] F. Luis, F. L. Mettes, J. Tejada, D. Gattesci, and L. J. de Jongh, Phys. Rev. Lett. **85**, 4377 (2000).

[31] M. Hennion, L. Pardi, I. Mirebeau, E. Suard, R. Sessoli, and A. Caneschi, Phys. Rev. B **56**, 8819 (1997).

[32] I. Mirebeau, M. Hennion, H. Caselto, H. Andres, H. Gudel, A. V. Irodova, and A. Caneschi, Phys. Rev. Lett. **83**, 628 (1999).

[33] Y. Zhong, M. P. Sarachik, J. P. Friedman, R. A. Robinson, T. M. Kelley, H. Nakotte, A. C. Christianson, F. Trouw, S. M. Aubin, and D. N. Hendrickson, J. Appl. Phys. **85**, 5636 (1999).

[34] R. A. Robinson, P. J. Brown, D. N. Argyriou, D. N. Hendrickson, and S. M. Aubin, J. Phys.: Condens. Matter **12**, 2805 (2000).

[35] A. L. Barra, D. Gatteschi, and R. Sessoli, Phys. Rev. B **56**, 8192 (1997).

[36] S. Hill, J. A. A. J. Perenboom, N. S. Dalal, T. Hathaway, T. Stalcup, and J. S. Brooks, Phys. Rev. Lett. **80**, 2453 (1998).

[37] A. Lascialfari, D. Gatteschi, F. Borsa, A. Shastri, Z. H. Jang, and P. Carretta, Phys. Rev. B **57**, 514 (1998); A. Lascialfari, Z. H. Jang, F. Borsa, P. Carretta, and D. Gatteschi, Phys. Rev. Lett. **81**, 3773 (1998); R. M. Achey, P. L. Kuhn, A. P. Reyes, W. E. Moulton, and N. S. Dulal, Phys. Rev. B **64**, 064420 (2001).

[38] Z. H. Jang, A. Lascialfari, F. Borsa, and D. Gatteschi, Phys. Rev. Lett. **84**, 2977 (2000).

[39] B. Barbara, W. Wernsdorfer, L. C. Sampaio, J. G. Park, C. Paulsen, M. A. Novak, R. Ferre, D. Mailly, R. Sessoli, A. Can-

eschi, K. Hasselbach, A. Benoit, and L. Thomas, J. Magn. Magn. Mater. **140–141**, 1825 (1955).
[40] M. A. Novak and R. Sessoli, in *Quantum Tunneling of Magnetization*, edited by L. Gunter and B. Barbara (Kluwer, Dordrecht, 1995).
[41] M. I. Katsnelson, V. V. Dobrovitski, and B. N. Harmon, Phys. Rev. B **59**, 6919 (1999).
[42] A. K. Zvezdin, V. V. Dobrovitski, B. N. Harmon, and M. I. Katsnelson, Phys. Rev. B **58**, 14 733 (1998).
[43] T. Goto, T. Kubo, T. Koshiba, Y. Fujii, A. Oyamada, J. Arai, K. Takeda, and K. Awaga, Physica B **284–288**, 1227 (2000).
[44] T. Kubo, T. Koshiba, T. Goto, A. Oyamada, Y. Fujii, K. Takeda, and K. Awaga, Physica B **294–295**, 310 (2001).
[45] A. Abragam and B. Bleaney, *Electron Paramagnetic Resonance of Transition Metal Ions* (Clarendon, Oxford, 1970).
[46] A. J. Freeman and R. E. Watson, in *Magnetism IIA*, edited by G. T. Rado and H. Suhl (Academic, New York 1965).
[47] T. Kubo, A. Hirai, and H. Abe, J. Phys. Soc. Jpn. **26**, 1094 (1969).
[48] H. J. G. Geritsen and E. S. Sabisky, Phys. Rev. **132**, 1507 (1963).
[49] T. Kubo and H. Yamahaku, Phys. Rev. B **32**, 1831 (1985).
[50] K. Takeda, K. Awaga, and T. Inabe, Phys. Rev. B **57**, 11 062 (1998).
[51] T. Kubo, H. Yasuoka, and A. Hirai, J. Phys. Soc. Jpn. **21**, 812 (1966).
[52] Y. Furukawa, K. Watanabe, K. Kumagai, F. Borsa, and D. Gatteschi, Phys. Rev. B **64**, 104401 (2001).
[53] T. Ohm, C. Sangregorio, and C. Paulsen, J. Low Temp. Phys. **113**, 1141 (1998); W. Wernsdorfer, T. Ohm, C. Sangregorio, R. Sessoli, D. Mailly, and C. Paulsen, Phys. Rev. Lett. **82**, 3903 (1999).
[54] B. Barbara (private communication).